THE OFFICIAL MAGAZINE OF THE OCEANOGRAPHY SOCIETY

Oceanography

CITATION

Crawford, A.J., P. Wadhams, T.J.W. Wagner, A. Stern, E.P. Abrahamsen, I. Church, R. Bates, and K.W. Nicholls. 2016. Journey of an Arctic ice island. *Oceanography* 29(2):254–263, http://dx.doi.org/10.5670/oceanog.2016.30.

DOI

http://dx.doi.org/10.5670/oceanog.2016.30

Photo credit:
Chris Packham

Journey of an Arctic Ice Island

By Anna J. Crawford, Peter Wadhams, Till J.W. Wagner, Alon Stern, E. Povl Abrahamsen, Ian Church, Richard Bates, and Keith W. Nicholls

ABSTRACT. In August 2010, a 253 km^2 ice island calved from the floating glacial tongue of Petermann Glacier in Northwest Greenland. Petermann Ice Island (PII)-B, a large fragment of this original ice island, is the most intensively observed ice island in recent decades. We chronicle PII-B's deterioration over four years while it drifted more than 2,400 km south along Canada's eastern Arctic coast, investigate the ice island's interactions with surrounding ocean waters, and report on its substantial seafloor scour. Three-dimensional sidewall scans of PII-B taken while it was grounded 130 km southeast of Clyde River, Nunavut, show that prolonged wave erosion at the waterline during sea ice-free conditions created a large underwater protrusion. The resulting buoyancy forces caused a 100 m × 1 km calving event, which was recorded by two GPS units. A field team observed surface waters to be warmer and fresher on the side of PII-B where the calving occurred, which perhaps led to the accelerated growth of the protrusion. PII-B produced up to 3.8 gigatonnes (3.8×10^{12} kg) of ice fragments, known hazards to the shipping and resource extraction industries, monitored over 22 months. Ice island seafloor scour, such as a 850 m long, 3 m deep trench at PII-B's grounding location, also puts subseafloor installations (e.g., pipelines) at risk. This long-term and interdisciplinary assessment of PII-B is the first such study in the eastern Canadian Arctic and captures the multiple implications and risks that ice islands impose on the natural environment and offshore industries.

INTRODUCTION

The floating ice tongue of Northwest Greenland's Petermann Glacier (PG) underwent extensive calving events in 2008, 2010, and 2012 (Peterson et al., 2009; Johannessen et al., 2011; Environment Canada, 2012). Each of these calvings created an immense ice island, with surface areas of 31 km^2 (Johannessen et al., 2011), 253 km^2 (Münchow et al., 2014), and 130 km^2 (Environment Canada, 2012), respectively. Since these calving events, a number of ice island fragments have been observed in regional waters such as Nares Strait, Baffin Bay, the Labrador Sea, and the Grand Banks (Figure 1a; Peterson et al., 2009; Halliday et al., 2012). Calving events such as these, together with increases in Canadian Arctic shipping (Pizzolato et al., 2014), and the likelihood of Baffin Bay hydrocarbon discoveries (National Energy Board, 2014), have renewed concerns regarding ice hazards in the eastern Canadian Arctic. These concerns are reinforced by the likely linkage between a warming climate and factors affecting calving fluxes, such as increased ocean temperatures, evolving seasonal mixed layer depths, decreasing protective sea ice extent, and increasing glacial velocities (Rignot and Kanagaratnam, 2006; Copland et al., 2007; Rignot and Steffen, 2008; Johnson et al., 2011; Moon et al., 2012).

Ice island field research has a longer history in the Beaufort and Chukchi Seas than in Baffin Bay, with long-term monitoring and sampling starting in the 1950s on ice islands originating from the northern Ellesmere Island ice shelves (Crary, 1958; Van Wychen and Copland, in press). Industrial interest spurred some of this research, which mostly came to an end in the early 1990s (Van Wychen and Copland, in press), though some more recent regional studies have been conducted (Copland et al., 2007; McGonigal et al., 2011; Mueller et al., 2013). Antarctic ice islands (which are referred to as tabular icebergs), such as those produced from the 2,240 km^2 Thwaites Glacier calving in 2010, have also been of research interest recently as a result of their contributions of freshwater and nutrients to ocean waters (MacGregor et al., 2012; Vernet et al., 2012; Smith et al., 2013). Unfortunately, ice island fieldwork in either polar region is logistically difficult, costly, and inherently dangerous to conduct, resulting in a paucity of information regarding ice island morphology, drift trajectories, and deterioration mechanisms (Enderlin and Hamilton, 2014; Crawford et al., 2015).

Petermann Ice Island (PII)-B, a large fragment of the August 5, 2010, PG calving event, is an exceptional example in this regard. The ice island was visited by two field expeditions within nine months,

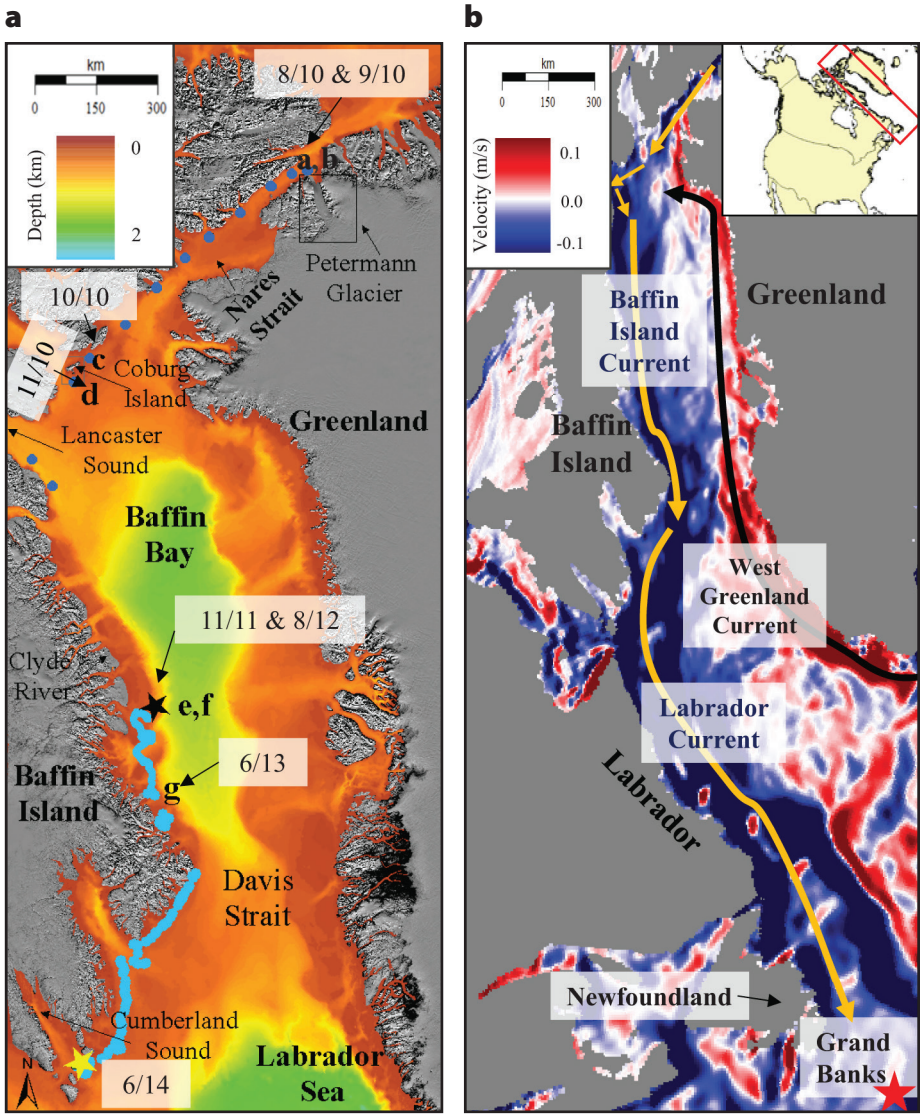

FIGURE 1. Regional overview maps and Petermann Ice Island (PII)-B drift. (a) Drift and locations of large fracture events of PII-B between August 2010 and June 2014. Lowercase letters a–g correspond to the satellite imagery series of Figure 2. Darker blue circles in the upper part of the figure indicate known locations of PII-B digitized from RADARSAT ScanSAR acquisitions as part of the Canadian Ice Island Drift and Deterioration Database (CI2D3, 2016; https://wirl.carleton.ca/research/ci2d3) between August and November 2010. GPS beacon locations are in light blue south of the grounding location denoted by the black star. The yellow star indicates the end of PII-B GPS monitoring. Bathymetry data are from the ETOPO2 data set (US Department of Commerce, 2006). Greenland, Baffin Island, and the Canadian Arctic Archipelago topography data are from the MEaSUREs MODIS Mosaic of Greenland 2005 (Haran et al., 2013). (b) Ocean meridional surface velocity (Griffies et al., 2009) and major currents along eastern Canada and western Greenland. The red star indicates the southernmost iceberg sighting for June–December 2014 (International Ice Patrol, 2015).

and its size and location were monitored for nearly four years (September 2010–June 2014) with satellite acquisitions and GPS beacons (Figure 1a). Fieldwork on PII-B was first conducted on October 23, 2011, from CCGS *Amundsen* (Hamilton et al., 2013). Further in situ data were collected between July 26 and August 3, 2012, during a field campaign based on M/V *Neptune* and run in conjunction with the British Broadcasting Corporation (BBC). This campaign later became the subject of the BBC television documentary "Operation Iceberg" (British Broadcasting Corporation, 2016).

Previous work has shown that the combination of fieldwork and remote-sensing data collection and analyses can prove an effective way to study ice island behavior (Martin et al., 2010). This paper uses such complementary remote-sensing and in situ data sets to meet three objectives. First, we use satellite observations and GPS data to chronicle the drift and large fractures that PII-B experienced throughout the four-year monitoring period. Second, we investigate how ocean forcings influenced its drift and deterioration. Finally, we assess the effect of the ice island on local bathymetry and the surrounding water column, and show how the latter likely contributed to the ice island's own deterioration.

THE HISTORY OF PII-B: DRIFT AND FRACTURE EVENTS

Data Collection

PII-B's motion and major fracturing events were monitored by satellite with ScanSAR and Fine-Quad (FQ) RADARSAT-2 acquisitions of 320 m and 8 m resolution, respectively, as well as Moderate Resolution Imaging Spectroradiometer (MODIS) imagery with 250 m resolution. Images of the fracture events are described below and shown in Figure 2. Single-frequency tracking beacons deployed in 2011 and 2012 also aided locational monitoring. Finally, the Operation Iceberg field team collected in situ data on PII-B's movement with successive multibeam sonar keel surveys using a Reson 8125 multibeam echosounder and two custom-built, geodetic-quality GPS units (Elosegui et al., 2012; Wagner et al., 2014) along with corresponding ocean velocity data collected with M/V *Neptune's* JRC JLN-628 Doppler current meter.

Trajectory and Fracture Events

PII-B was formed in September 2010 when the original 2010 ice island (Figure 2a) fractured after colliding with Joe Island at the mouth of Petermann Fjord (Figure 2b). The 160 km^2 PII-B fractured twice more during the following month, reducing its surface area by ~50% and creating five additional ice islands with surface areas between 2 km^2 and 28 km^2 (Figure 2c,d). PII-B continued drifting southward along Baffin Island's coast before grounding in June 2011 at 69.64°N, 65.85°W, 130 km southeast of Clyde River, Nunavut. Approximately one-third of the 59 km^2 PII-B (Figure 2e) calved off the main island six months later. Following this fracture event, PII-B, then 41 km^2 (Figure 2f), was observed to pivot noticeably about its grounding point. The cause of the pivot motion was

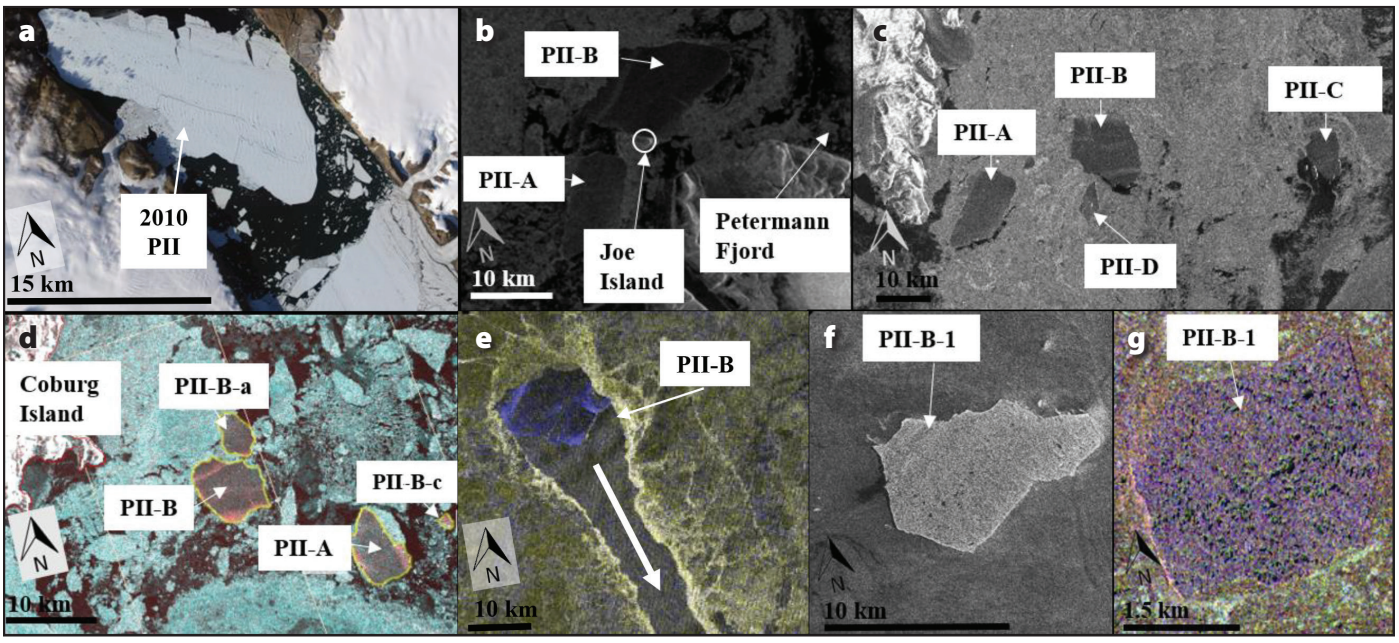

FIGURE 2. Chronology of formative events during PII-B monitoring as captured by (a) MODIS, (b) Envisat, and (c–g) RADARSAT-2 satellites. These events correspond to the labeled locations in Figure 1a. Dates: (a) August 16, 2010, (b) September 9, 2010, (c) October 12, 2010, (d) October 30, 2010, (e) November 13, 2011, (f) August 8, 2012, and (g) June 29, 2013. The arrow in (e) points to the sea ice wake observed during the November 2011 fracture event. Images are courtesy of NASA MODIS Earth Observatory (EO-1 ALI satellite), European Space Agency (Envisat), and Canadian Space Agency (RADARSAT-2).

explored with the GPS and current data. We found a strong relationship between the ice island's meridional motion from the GPS and the measured meridional currents (Figure 3a). Both data sets show clear semidiurnal cycles, covarying with the predicted tides from Arctic Ocean Tidal Inverse Model-5 (Padman and Erofeeva, 2004), a strong indicator that the oscillations illustrated in Figure 3b are tidally forced.

PII-B ungrounded and resumed drifting south in August 2012. By this time, the area of PII-B had been reduced to 12 km^2 (Figure 2g). Remote monitoring finished when both GPS beacons ceased transmitting on June 10, 2014, and PII-B was located at the mouth of Cumberland Sound (Figure 1a). PII-B traveled at an average speed of 0.71 km hr^{-1} during periods of drift after August 2012, with a maximum speed of 3.4 km hr^{-1}. PII-B experienced alternating periods of approximately one to three weeks of drift and immobility between August and December 2012, suggesting that the ice island became grounded for short periods on Baffin Island's continental shelf. The ice island then remained immobile between December 2012 and May 2013 when sea ice concentrations were high (Figure 4c) and it was likely trapped within fast ice. After this period, PII-B drifted almost continuously through June 2014. It can be assumed that PII-B completely deteriorated before reaching 43°N, based on the minimum latitude of the International Ice Patrol's iceberg sightings after June 10, 2014 (Figure 1b; International Ice Patrol, 2015).

Drift Influences and Comparisons to Previous Observations

PII-B and its fragments followed the usual trajectory of ice islands originating in Northwest Greenland (Newell, 1993), which involves drifting south through Nares Strait (Robeson and Kennedy Channels, Kane Basin, and Smith Sound) and into Baffin Bay and the Labrador Sea (Peterson et al., 2009; Peterson, 2011). Figure 1b shows the meridional velocity component of the regional surface currents from the 1/8th degree MOM6 global model, with dominant current directions indicated by arrows (Newell, 1993; Tang et al., 2004; Adcroft et al., 2010). Upon entering Baffin Bay, the ice island's drift is determined by the prevailing current in the top 300 m layer of "Arctic water," which is sourced from Nares Strait and runs along the bay's western edge (Tang et al., 2004). The ice islands are directed by the bay's cyclonic currents and continue south in the strong Baffin Current, following the shelf edge of Baffin Island. This current is strongest within 100 km of Baffin Island's coast (Fissel et al., 1982; Tang et al., 2004). Drift continues into the Labrador Sea with the Labrador

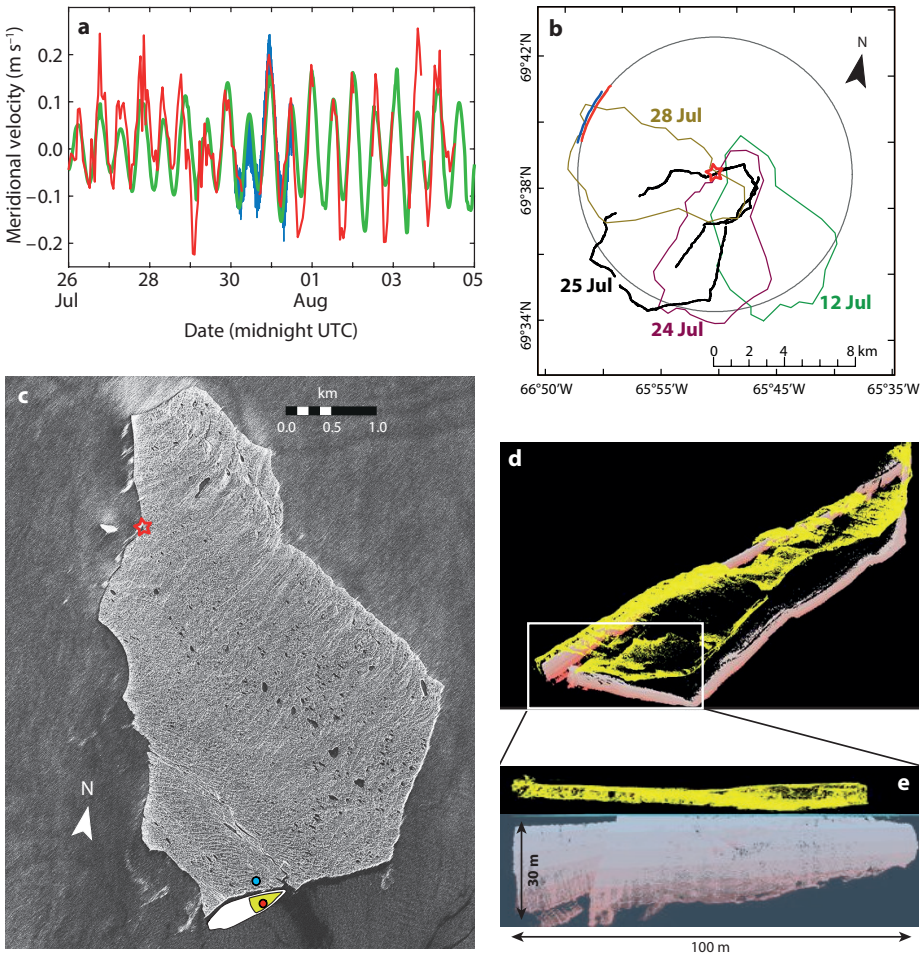

FIGURE 3. (a) Meridional currents at 50 m depth measured from the Doppler current meter on M/V *Neptune* (gaps in the red plot correspond to periods when the multibeam sonar was in use, resulting in interference between the two instruments), tidal currents from the AOTIM5 model at the ship's position (green; Padman and Erofeeva, 2004), and movement of the ice island as recorded by GPS (blue). (b) Ice island oscillation, represented by multiple outlines. The thick black outline is the multibeam survey, while the other outlines are digitized from MODIS. The red and blue lines are GPS tracks (July 30–31), and the black circle denotes the full, theoretical 360° path of the red GPS track. (c) PII-B as imaged with an ultra-fine (3 m resolution) RADARSAT-2 acquisition from August 1, 2012, with the approximate locations of the two GPS units (●, ●) and the grounding point (red star). The distance between the two units is approximately 210 m. The white polygon represents the shape of PII-B prior to the calving event. The section outlined in yellow roughly corresponds to the fragment illustrated in Figure 3d. (d) Three-dimensional multibeam sonar image (pink) and lidar scan (yellow) of the keel and freeboard, respectively, of the fragment portion outlined in yellow in Figure 3c. (e) A cross-sectional scan of the calved piece in Figure 3d. Color representation is the same as in (d). All RADARSAT-2 products are © MacDonald, Dettwiler and Associates Ltd. (2011–2013), all rights reserved. RADARSAT is an official mark of the Canadian Space Agency. *(b) is adapted from Figure 1 of Stern et al. (2015), (d) and (e) are adapted from Figures 1 and 2 of Wagner et al. (2014), all used with permission of John Wiley & Sons*

Current (Figure 1b; Newell, 1993) and on to Newfoundland's Grand Banks, the historical southern limit of iceberg drift as a result of the Northwest Atlantic's warmer waters (Tang et al., 2004; Peterson, 2011).

The time required for PG ice islands to travel to these southern limits is highly variable. Halliday et al. (2012) document PII-A's rapid 11-month transit over 3,000 km from PG to the Labrador coast, while PII-B took four years to drift approximately 2,400 km, even though both ice islands originated from the same calving event in 2010. Two main factors explain the prolonged stay of some ice islands at more northern latitudes: (1) extended incursions into adjoining waters, and (2) grounding on shallow bathymetry (Newell, 1993; Peterson, 2011). The departure of ice islands into Lancaster and Jones Sounds has been previously documented (Peterson, 2011), and can be explained by the strong coastal current inflow encountered when approaching from the north (Figure 1b; Fissel et al., 1982; Tang et al., 2004). Iceberg drift models indicate the momentum balance is dominated by (1) water drag, and (2) the ageostrophic pressure gradient force. (Because icebergs move principally with ocean currents, the Coriolis force on an iceberg is largely canceled out by the geostrophic part of the pressure gradient force, and the residual is dominated by the ageostrophic pressure gradient force). These forces together are estimated to amount to ~70% of the forces dictating iceberg motion (Bigg et al., 1997; Savage, 2001). The importance of the ageostrophic pressures has been attributed to the strong seasonal variability and horizontal shear flows in the Labrador and Greenland Seas (Bigg et al., 1996, 1997). While water drag and ageostrophic pressures dominate, large wind events can also play a role in directing iceberg drift trajectories. It is likely that large easterly wind events are responsible for many of the ice island groundings along Baffin Island's shallow continental shelf, such as PII-B's own 15-month grounding period (G. Crocker and R. Saper, Carleton University, *pers. comm.*, February 2016). The following sections focus specifically on this segment of PII-B's life history.

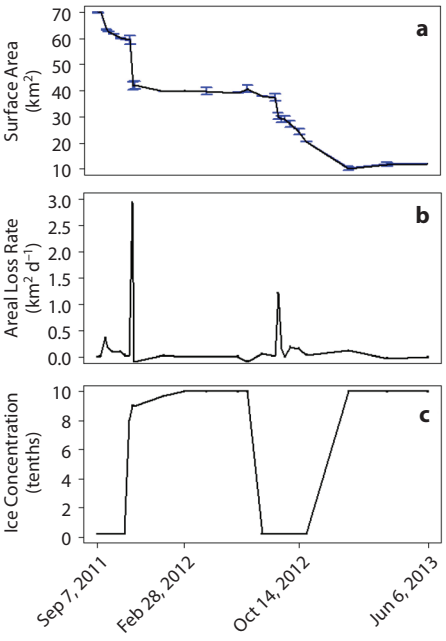

FIGURE 4. PII-B deterioration during the RADARSAT-2 Fine-Quad monitoring period: (a) surface area, (b) areal loss rate, and (c) sea ice concentration.

OCEANOGRAPHIC INFLUENCES ON PII-B'S DETERIORATION

The oceanographic conditions that an ice island encounters will affect its deterioration rate. Here, we investigate how oceanographic factors (e.g., buoyancy forces and wave erosion) and sea ice concentrations influenced PII-B's deterioration. We also assess total mass loss during a subset of this time to provide an estimate of the mass of ice hazards and freshwater input generated by PII-B.

Observation Techniques and Mass Calculation Methods

The surface area of PII-B was monitored from September 7, 2011, to June 29, 2013, by digitizing the ice island's perimeter using high-resolution RADARSAT-2 FQ imagery. Ice island thickness was estimated by assuming a constant basal melt rate and using a surface melt rate proportional to air temperature (Hock, 2003; Enderlin and Hamilton, 2014). We used air temperature data generated by the Global Environmental Multiscale model, which is used for operational modeling at the Canadian Ice Service. We used a basal melt rate of 1.3 cm d^{-1} based on in situ measurements collected around PII-B, and a surface melt rate of 0.64 cm d^{-1} $°C^{-1}$ above freezing, following Stern et al. (2015) and Crawford et al. (2015), respectively. Thickness changes were referenced to the average 70 ± 10 m thickness derived during 2012 Operation Iceberg fieldwork (Wagner et al., 2014). Ice island mass was estimated using a density of 890 kg m^{-3}.

Sea ice concentration data (in tenths) were collected from polygon shapefiles gathered from the Canadian Ice Service (CIS) archives to evaluate how sea ice was implicated in areal deterioration. Figure 4a shows the surface area of PII-B, and Figure 4b and 4c show the areal loss rate and sea ice concentrations, respectively. Uncertainties in these measurements are estimated using the "equivalent-area square" method (Ghilani, 2000), in which the uncertainty in digitized surface area is computed by varying product resolutions and ice island size (see error bars in Figure 4a, ranging from 0.01 km^2 to 2.86 km^2).

Wave Erosion, Sea Ice, and Ice Island Deterioration

The surface area of PII-B reduced by 58 km^2 over the 22-month monitoring period (Figure 4a). Modeled thickness change showed a decrease of 12 m, with basal ablation responsible for ~70% of this thinning. After accounting for surface and basal ablation, roughly 3.8 gigatonnes (3.8×10^{12} kg) of mass was lost through large fracturing, small calving, or sidewall melt. A comparison of Figure 4b and 4c illustrates that almost all of the surface area reduction occurred when no sea ice was present.

Sea ice was not present when the Operation Iceberg field team observed PII-B calving a ~100 m × 1 km fragment in July 2012 (Figure 3c). Data recorded

by the two GPS units showed the calved piece rose abruptly by 63.1 ± 0.4 cm after the breakup relative to the main ice island. The calving, and possibly other large fracturing events of PII-B, were likely induced by substantial local hydrostatic imbalances caused by a protruding underwater "foot" that was observed in the lidar and multibeam scans (Figure 3d,e). This foot imparted an upward force due to its buoyancy, resulting in a net local bending stress on the main island, which ultimately led to the observed fracture and the rise of the calved piece. Wagner et al. (2014) described this process as the "footloose mechanism," and it is similar to observations of Antarctic iceberg deterioration (Scambos et al., 2005). This process becomes important when an ice island enters warm, sea ice-free waters. The presence of sea ice dampens surface waves (Squire, 2007), which protect an ice island's sidewalls. Without this barrier, the rate of wave-induced erosion at the waterline increases. This process creates a notch, after which unsupported sidewalls calve, leading to the development of the submerged protrusion described above (Savage, 2001). Scambos et al. (2008) also observed that large fracturing and rapid deterioration events only occurred to a tabular Antarctic iceberg when it was in open-water conditions, while slower rates of decay occurred when the ice feature was enclosed by sea ice.

PII-B also experienced two large fracture events while monitored by RADARSAT-2. These events are indicated in Figure 4b by large spikes in surface area loss rate. The November 2011 fracturing event was responsible for 80% of the areal reduction observed between field campaigns. The second fracture occurred between August 27 and September 2, 2012, when PII-B's area was reduced by a further 7.3 km^2 to 30.2 km^2 (Figure 4a). The second event clearly occurred during sea ice-free conditions, while the first occurred in partial sea ice cover (Figure 4b,c). Interestingly, a ScanSAR image taken on November 13, 2011, (Figure 2e), before this calving event, shows a large wake in the sea ice forming down-current from the ice island. This wake is not captured in the CIS regional sea ice chart. The area of open water abutted the region of PII-B that eventually calved three days later on November 16, 2011.

> "This case study of a single ice island during its journey through Nares Strait and Baffin Bay illustrates the varied forces and processes that can influence ice island drift and deterioration, as well as the varied risks that these immense ice hazards pose to offshore industries."

CONSEQUENCES OF ICE ISLAND GROUNDING ON LOCAL BATHYMETRY AND THE WATER COLUMN

An ice island's presence can affect the adjacent water column and local seafloor topography. Here, we focus on the influences exerted by PII-B on its surroundings while grounded in Baffin Bay.

Data Collection

Seabed Morphology

Changes to seabed morphology caused by the rotation and grounding of PII-B were examined with overlapping multibeam sonar data sets acquired pre- and post-grounding of PII-B. Serendipitously, baseline seabed morphology was obtained before PII-B's grounding when CCGS *Amundsen* transited near the site in 2005 during a routine tour of the Canadian Arctic Archipelago. The ship is equipped with a Kongsberg Maritime EM302 30 kHz multibeam sonar system that collects data continuously while underway (Muggah et al., 2010). The site was revisited in 2013 for a more thorough seabed survey by CCGS *Amundsen* to investigate the potential effect of the ice island grounding on the surrounding seabed.

Local Effects on Water Column

To explore possible upwelling and downwelling patterns in the water column arising from the grounded ice island, a series of conductivity-temperature-depth (CTD) casts were taken between July 25 and July 29, 2012, around PII-B during the Operation Iceberg field campaign. An ADM mini-CTD probe was used during five transects, moving radially outward from the ice island, starting and ending approximately 1 km and 10 km from PII-B's edge, respectively. Data acquired from the ship-borne Doppler current meter were used in the subsequent analyses. GPS data recorded by the ship and units deployed on PII-B were used to monitor drift during the observation period. Wind-driven upwelling was modeled with both in situ data and the European Centre for Medium-Range Weather Forecasts' daily ERA-Interim reanalysis (Dee et al., 2011; see Stern et al., 2015, for further details).

Morphological Consequences of Grounding on the Seabed

Overlaying the approximate PII-B grounding pivot point onto the multibeam bathymetry shows the ice island was grounded on a shoal with a depth of approximately 96 m (referenced to mean sea level; Figure 5a). Comparing the 2005 and 2013 bathymetry reveals a scour line south of the grounding site incised to approximately 3 m below the 2005 seabed, to a depth of 93 m (Figure 5b). The width of scour is approximately 100 m, which is at the upper end of common iceberg scour widths described by Dowdeswell

et al. (1992), and it continues for 850 m from the pivot point over the shoal. The scour disappears at a depth of 92 m as the seabed deepens toward the south.

Knowledge of possible rates, locations, and sizes of scours is important for the design of subseafloor installations in regions of interest to the offshore natural resource extraction industry. Historically, attention was focused on the Labrador Sea and North Atlantic regions because of the extraction projects underway on Newfoundland's Grand Banks (Fuglem et al., 1996; King et al., 2009) and within the Labrador Sea (Todd et al., 1988), although iceberg scour surveys have also been conducted in eastern Canada to study the outpouring of icebergs during Heinrich Events from the Laurentide Ice Sheet during the last glaciation (Metz et al., 2008).

Industrial concern also provides the main impetus for scour assessments in the Beaufort Sea (McGonigal et al., 2011; Fuglem and Jordaan, in press), where ice islands are possible hazards as they drift within the Beaufort Gyre after calving from northern Ellesmere Island ice shelves (Mueller et al., 2013). Moving ice islands have greater momentum than smaller icebergs because of their substantial mass, and, as exemplified by the observed scour caused by PII-B, they can create deep and wide scours that would be devastating to seafloor-mounted infrastructure. These scours can be either curved or relatively straight, depending on the local dominance of rotary tidal currents or translatory ocean currents, respectively (Todd et al., 1988), and the influence of both on scour regimes should be considered when planning seafloor installations along the Baffin Island continental shelf and elsewhere in the Arctic region.

Oceanographic Upwelling and Downwelling Around PII-B

In addition to the visible modification to local seafloor topography, the presence of a grounded ice island was found to alter the stratification of the surrounding ocean. An analysis of the 2012 PII-B CTD casts showed that the top 15 m of the water column was warmer and fresher on the southwest side of the ice island than on the northeast side (Figure 6). On the northeastern CTD transect, the isopycnals were observed to slope upward toward the ice island, suggesting that cooling on this side of the ice island was caused by cool saline water upwelling from below. On the southern side of the ice island, the warm, fresh surface water is accompanied by a sharpening of the thermocline separating the warm fresh water in the mixed layer from the cool salty water below. Stern et al. (2015) suggest that a wind-driven surface Ekman current moving 90° to the right of the wind direction can explain these observations. On one side of the ice island, this causes the surface water to move away from the ice edge and results in upwelling of the water below. The warm fresh surface water moves toward the ice

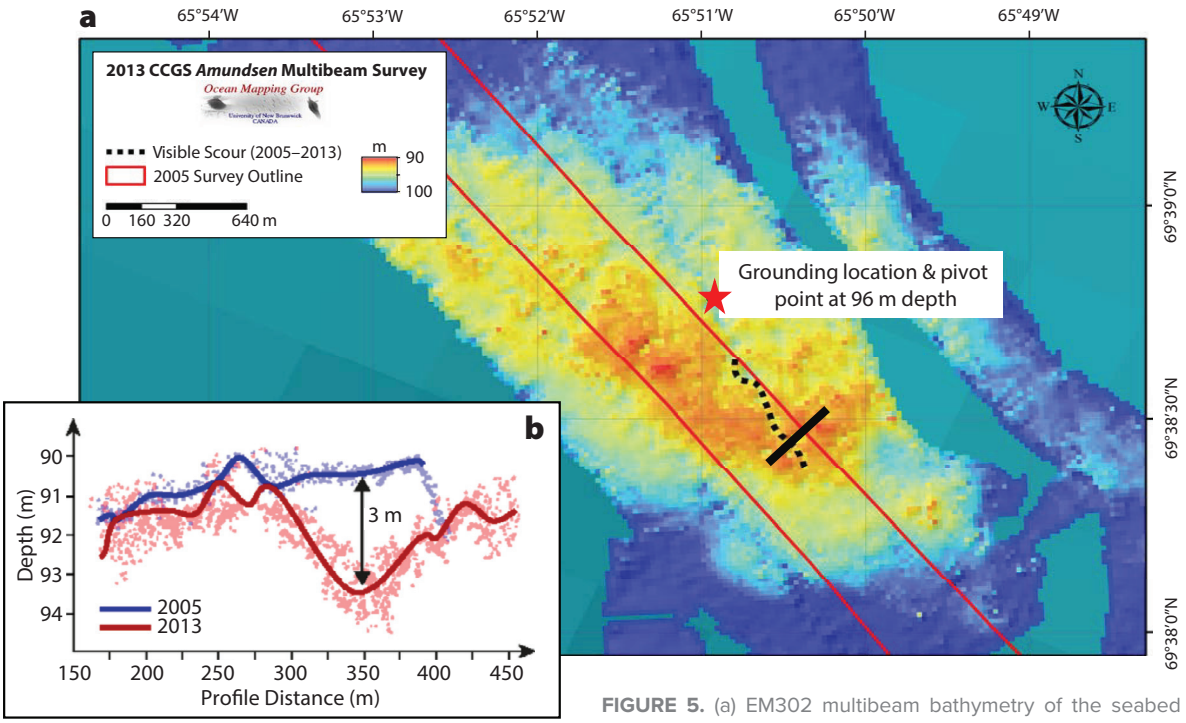

FIGURE 5. (a) EM302 multibeam bathymetry of the seabed surrounding the PII-B grounding site (Figure 1a). The bathymetry grid is derived from a 2013 survey after the departure of PII-B, while the red lines depict the extent of the 2005 CCGS *Amundsen* multibeam data corridor. The dashed black line depicts the location of a scour generated between 2005 and 2013 and follows south of the grounding location. The solid black line represents the location of the profile shown in (b). (b) Representative east-west two-dimensional profile across the seabed scour generated by PII-B. Vertical exaggeration is set to 60x to emphasize the scour.

island on the opposite side, piling up at the sidewall and causing a sharpening of the thermocline (Figure 6). This mechanism suggests that, over time, an ice island should erode fastest on the side to the left of the prevailing wind direction, while the opposite side should decay more slowly because of the cool surface waters caused by ocean upwelling. The grounded ice island can thus be expected to modify the spatial distribution of its own deterioration. Evidence for this process was seen in the satellite imagery of PII-B acquired between January and September 2012, which showed that >75% of PII-B's areal deterioration occurred in the southern quadrant of the ice island, while this quadrant represented only 25% of the ice island's perimeter (Figure 6). This is also the location of the observed footloose-style fracture discussed above. The prevailing wind direction was toward the west during this time period, meaning that the expedited decay on the southern side of the iceberg was consistent with the mechanism suggested by Stern et al. (2015).

SYNTHESIS, CONCLUSIONS, AND FUTURE WORK

A 253 km^2 ice island calved from the floating ice tongue of Petermann Glacier on August 5, 2010. Petermann Ice Island-B, the largest fragment of the original ice island, was monitored over a four-year period from the time of calving until it reached the mouth of Cumberland Sound in 2014. During this period, PII-B was observed using satellite imagery, tracked by GPS, and visited by two separate field experiments, making it the most intensively studied ice island in recent history. This is the first long-term study of an individual ice island in the eastern Canadian Arctic, following the shorter-duration analyses of Forrest et al. (2012), Halliday et al. (2012), and Crawford et al. (2015). The objectives of this study were to: (1) chronicle PII-B's drift and large fracture events, (2) determine how ocean forcings influenced this drift and deterioration, and (3) assess how PII-B affected local bathymetry and its own deterioration by altering the surrounding ocean column.

PII-B drifted through Nares Strait and western Baffin Bay, a similar route to other ice islands sourced from Northwest Greenland's floating ice tongues and ice shelves (Newell, 1989; Peterson, 2011). PII-B's southern drift was delayed by a 15-month grounding period 130 km southeast of Clyde River, Nunavut. While grounded, PII-B was observed to rotate about its grounded point, moving in phase with tidal motion. Repeat bathymetry surveys (before and after grounding) also revealed a 3 m deep, 100 m wide, and 850 m long seafloor scour emanating from the grounding location. Further statistical or empirical analyses are needed to predict common grounding zones along Baffin Island's continental shelf. Prior research has focused on iceberg scour at more southern latitudes (King et al., 2009); however, it is likely that other ice islands have left similar marks in the region and future scour could be devastating to subseafloor installations used for offshore resource extraction.

PII-B fractured on a number of occasions while adrift in the eastern Canadian Arctic, creating numerous smaller icebergs, all of which are potential hazards to vessels and offshore structures. By monitoring PII-B's areal deterioration and accounting for thickness change, we estimate that the mass of ice hazards that PII-B generated while drifting in Baffin Bay was 3.8 gigatonnes (3.8×10^{12} kg) over the course of 22 months. This information can be used by offshore stakeholders

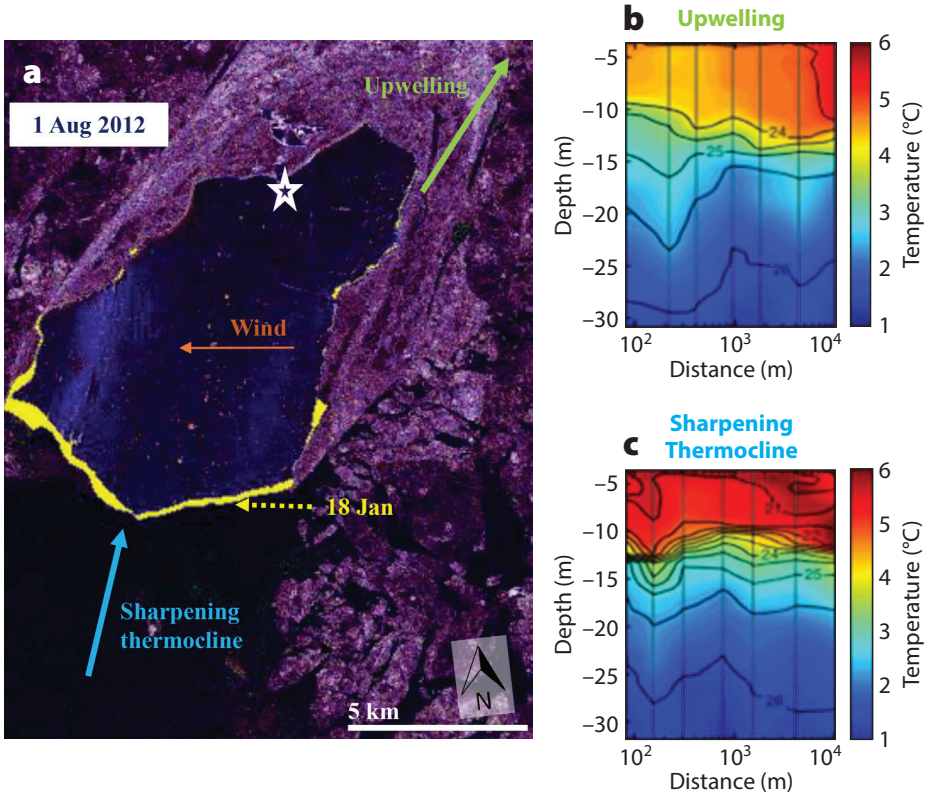

FIGURE 6. (a) Surface area comparison between January 18, 2012 (yellow outline, digitized from an acquired RADARSAT-2 FQ image), and August 1, 2012 (RADARSAT-2 FQ image shown), illustrating the preferential deterioration of PII-B in the vicinity of the observed sharpening thermocline while grounded (red star). PII-B decreased by 1.8 km^2 in surface area during this period. Temperature sections from CTD casts along transects, noted by the colored arrows, on opposing sides of PII-B-1 showed upwelling (b) and thermocline sharpening (c) to the right and left, respectively, of the predominate wind direction denoted in (a). All RADARSAT-2 products are © MacDonald, Dettwiler and Associates Ltd. (2011–2013), all rights reserved. RADARSAT is an official mark of the Canadian Space Agency. *(b) and (c) are modified from Figure 4 of Stern et al. (2015), used with permission of John Wiley & Sons*

to approximate the maximum mass of ice hazards generated from a single, large ice island in the region. This is similar to the hazard production estimates for smaller icebergs by Crocker et al. (2004).

The wave-enhanced sidewall deterioration that was implicated in the footloose and thermal stratification deterioration mechanisms affects how freshwater is released into the ocean, which may carry important consequences for the surrounding marine environment (Smith et al., 2013). While research has been conducted on freshwater input magnitudes and ecosystem impacts of deteriorating ice islands in the Antarctic (Vernet et al., 2012), this work has not been performed at the same scale for the Arctic (Smith et al., 2013) and is a subject needing further research.

Additionally, further data collection via field and remote-sensing campaigns are necessary to continue augmenting drift and deterioration databases. In situ data collection regarding drift velocities and melt magnitudes with varying environmental conditions (e.g., wave amplitudes, temperatures, and wind and ocean currents) is necessary for improving numerical models, while remote-sensing data collection can be used for statistical analyses of large fracturing events. We show the complementarity of these data sets in the intensive study of PII-B. This case study of a single ice island during its journey through Nares Strait and Baffin Bay illustrates the varied forces and processes that can influence ice island drift and deterioration, as well as the risks that these immense ice hazards pose to offshore industries.

REFERENCES

Adcroft, A., R. Hallberg, J.P. Dunne, B.L. Samuels, J.A. Galt, C.H. Barker, and D. Payton. 2010. Simulations of underwater plumes of dissolved oil in the Gulf of Mexico. *Geophysical Research Letters* 37, L18605, http://dx.doi.org/10.1029/2010GL044689.

Bigg, G.R., M.R. Wadley, D.P. Stevens, and J.A. Johnson. 1996. Prediction of iceberg trajectories in the North Atlantic and Arctic Oceans. *Geophysical Research Letters* 23:3,587–3,590, http://dx.doi.org/10.1029/96GL03369.

Bigg, G.R., M.R. Wadley, D.P. Stevens, and J.A. Johnson. 1997. Modelling the dynamics and thermodynamics of icebergs. *Cold Regions Science and Technology* 26:113–135, http://dx.doi.org/10.1016/S0165-232X(97)00012-8.

British Broadcasting Corporation. 2016. BBC2: Operation Iceberg home page, http://www.bbc.co.uk/programmes/p00tvcnx.

CI2D3 (Canadian Ice Island Drift and Deterioration Database). 2016. Canadian Ice Island Drift and Deterioration Database Final Report. Prepared by the Water and Ice Research Lab for the Canadian Ice Service, Environment Canada, 13 pp.

Copland, L., D.R. Mueller, and L. Weir. 2007. Rapid loss of the Ayles Ice Shelf, Ellesmere Island, Canada. *Geophysical Research Letters* 34, L21501, http://dx.doi.org/10.1029/2007GL031809.

Crary, A.P. 1958. Arctic ice island and ice shelf studies: Part 1. *Arctic* 11(1):1–68.

Crawford, A., D.R. Mueller, E.R. Humphreys, T. Carrieres, and H. Tran. 2015. Surface ablation model evaluation on a drifting ice island in the Canadian Arctic. *Cold Regions Science and Technology* 110:170–182, http://dx.doi.org/10.1016/j.coldregions.2014.11.011.

Crocker, G., J. English, R. McKenna, and R. Gagnon. 2004. Evaluation of bergy bit populations on the Grand Banks. *Cold Regions Science and Technology* 38:239–250, http://dx.doi.org/10.1016/j.coldregions.2003.12.001.

Dee, D.P., S.M. Uppala, A.J. Simmons, P. Berrisford, P. Poli, S. Kobayashi, U. Andrae, M.A. Balmaseda, G. Balsamo, P. Bauer, and others. 2011. The ERA-Interim reanalysis: configuration and performance of the data assimilation system. *Quarterly Journal of the Royal Meteorological Society* 137:553–597, http://dx.doi.org/10.1002/qj.828.

Dowdeswell, J.A., R.J., Whittington, and R. Hodgkins. 1992. The sizes, frequencies, and freeboards of East Greenland icebergs observed using ship radar and sextant. *Journal of Geophysical Research* 97(C3):3,515–3,528, http://dx.doi.org/10.1029/91JC02821.

Elosegui, P., J. Wilkinson, M. Olsson, S. Rodwell, A. James, B. Hagan, B. Hwang, R. Forsberg, R. Gerdes, J. Johannessen, and others. 2012. High-precision GPS autonomous platforms for sea ice dynamics and physical oceanography. Abstract C13E-066 presented at 2012 Fakk Meeting, American Geophysical Union, San Francisco, CA, December 3–7.

Enderlin, E.M., and G.S. Hamilton. 2014. Estimates of iceberg submarine melting from high-resolution digital elevation models: Application to Sermilik Fjord, East Greenland. *Journal of Glaciology* 60(224):1,084–1,092, http://dx.doi.org/10.3189/2014JoG14J085.

Environment Canada. 2012. Petermann Glacier Ice Island 2012, http://www.ec.gc.ca/default.asp?lang=En&n=592AB94B-1&news=63B51150-B0B0-438F-94CA-A1CDDFA86A25.

Fissel, D.B., D.D. Lemmon, and J.R. Birch. 1982. Major features of the summer near-surface circulation of western Baffin Bay, 1978–1979. *Arctic* 35(1):180–200.

Fuglem, M., I. Jordaan, G. Crocker, G. Cammaert, and B. Berry. 1996. Environmental factors in iceberg collision risks for floating systems. *Cold Regions Science and Technology* 24(3):251–261, http://dx.doi.org/10.1016/0165-232X(95)00013-2.

Fuglem, M., and I. Jordaan. In press. Risk analysis and hazards of ice islands. In *Arctic Ice Shelves and Ice Islands.* L. Copland and D. Mueller, eds, Springer, New York, NY.

Ghilani, C.D. 2000. Demystifying area uncertainty: More or less. *Surveying and Land Information Systems* 60:177–182.

Griffies, S.M., A. Biastoch, C. Böning, F. Bryan, G. Danabasoglu, E.P. Chassignet, M.H. England, R. Gerdes, H. Haak, R. W. Hallberg, and others. 2009. Coordinated Ocean ice Reference Experiments (COREs). *Ocean Modelling* 26(1–2):1–46, http://dx.doi.org/10.1016/j.ocemod.2008.08.007.

Halliday, E.J., T. King, P. Bobby, L. Copland, and D. Mueller. 2012. Petermann Ice Island 'A' survey results, offshore Labrador. *Proceedings of the Arctic Technology Conference*, December 3–5, 2012, Houston, TX, OTC 23714.

Hamilton, A.K., A.L. Forrest, A. Crawford, V. Schmidt, B.E. Laval, D.R. Mueller, S. Brucker, and T. Hamilton. 2013. *Project ICEBERGS Final Report*. Report prepared for the Canadian Ice Service, Environment Canada, 36 pp.

Haran, T., J. Bohlander, T. Scambos, T. Painter, and M. Fahnestock. 2013. MEaSUREs MODIS Mosaic of Greenland 2005 (MOG2005) Image Map, Version 1. Boulder, Colorado. NSIDC: National Snow and Ice Data Center, http://dx.doi.org/10.5067/IAGYM8Q26QRE.

Hock, R. 2003. Temperature index melt modeling in mountain areas. *Journal of Hydrology* 282(1–4):104–115, http://dx.doi.org/10.1016/S0022-1694(03)00257-9.

International Ice Patrol. 1995, updated 2015. International Ice Patrol (IIP) Iceberg Sightings Database, Version 1. Boulder, Colorado USA: National Snow and Ice Data Center/World Data Center for Glaciology, http://dx.doi.org/10.7265/N56Q1V5R.

Johannessen, O.M., M. Babiker, and M.W. Miles. 2011. Petermann Glacier, North Greenland: Massive calving in 2010 and the past half century. *The Cryosphere Discussions* 5:169–181, http://dx.doi.org/10.5194/tcd-5-169-2011.

Johnson, H.L., A. Münchow, K.K. Falkner, and H. Melling. 2011. Ocean circulation properties in Petermann Fjord, Greenland. *Journal of Geophysical Research* 116, C01003, http://dx.doi.org/10.1029/2010JC006519.

King, T., R. Phillips, J. Barrett, and G. Sonnichsen. 2009. Probabilistic pipeline burial analysis for protection against ice scour. *Cold Regions Science and Technology* 59:58–64, http://dx.doi.org/10.1016/j.coldregions.2009.05.013.

MacGregor, J.A., G.A. Catania, M.S. Markowski, and A. Andrews. 2012. Widespread rifting and retreat of ice-shelf margins in the eastern Amundsen Sea Embayment between 1972 and 2011. *Journal of Glaciology* 58(209):458–466, http://dx.doi.org/10.3189/2012JoG11J262.

Martin, S., R. Drucker, R. Aster, F. Davey, E. Okal, T. Scambos, and D. MacAyeal. 2010. Kinematic and seismic analysis of giant tabular iceberg breakup at Cape Adare, Antarctica. *Journal of Geophysical Research* 115, B06311, http://dx.doi.org/10.1029/2009JB006700.

McGonigal, D., D. Hagen, and L. Guzma. 2011. Extreme ice features distribution in the Canadian Arctic. *Proceedings of the 20th International Conference on Port and Ocean Engineering Under Arctic Conditions,* July 11–14, 2011, Montréal, Quebec, Canada, POAC 11-045.

Metz, J.M., J.A. Dowdeswell, and C.M.T. Woodworth-Lynas. 2008. Sea-floor scour at the mouth of Hudson Strait by deep-keeled icebergs from the Laurentide Ice Sheet. *Marine Geology* 253:149–159.

Moon, T., I. Joughin, B. Smith, M.R. van den Broeke, W.J. van de Berg, B. Noel, and M. Usher. 2012. Distinct patterns of seasonal Greenland glacier velocity. *Geophysical Research Letters* 41(20):7,209–7,216, http://dx.doi.org/10.1002/2014GL061836.

Mueller, D., A. Crawford, L. Copland, and W. Van Wychen. 2013. *Ice Island and Iceberg Fluxes from Canadian High Arctic Sources.* Report prepared for the Northern Transportation Assessment Initiative, Innovation Policy Branch, Transport Canada, Ottawa, Ontario, Canada, 22 pp.

Muggah, J., I. Church, J. Beaudoin, and J.E. Hughes Clarke. 2010. Seamless Online Distribution of Amundsen Multibeam Data. Paper S7.2 in *Proceedings of the Canadian Hydrographic Conference*, 19 pp.

Münchow, A., L. Padman, and H.A. Fricker. 2014. Interannual changes of the floating ice shelf of Petermann Gletscher, North Greenland, from 2000 to 2012. *Journal of Glaciology* 60(221):489–499, http://dx.doi.org/10.3189/2014JoG13J135.

National Energy Board. 2014. Environmental Assessment Report for the Northeastern Canada 2D Seismic Survey (Baffin Bay/Davis Strait), 36 pp.

Newell, J.P. 1993. Exceptionally large icebergs and ice islands in Eastern Canadian waters: A review of sightings from 1900 to present. *Arctic* 46(3):205–211.

Padman, L., and S. Erofeeva. 2004. A barotropic inverse tidal model for the Arctic Ocean. *Geophysical Research Letters* 31, L02303, http://dx.doi.org/10.1029/2003GL019003.

Peterson, I.K. 2011. Ice island occurrence on the Canadian East Coast. *Proceedings of the International Conference on Port and Ocean Engineering under Arctic Conditions*, July 10–14, 2011, Montréal, Quebec, Canada, POAC11-044.

Peterson, I.K., S.J. Prinsenberg, M. Pittman, and L. Desjardins. 2009. The drift of an exceptionally large ice island from the Petermann Glacier in 2008. *Proceedings of the 20th International Conference on Port and Ocean Engineering under Arctic Conditions,* June 9–12, 2009, Luleå, Sweden, POAC09-130.

Pizzolato, L., S.E.L. Howell, C. Derksen, J. Dawson, and L. Copland. 2014. Changing sea ice conditions and marine transportation activity in Canadian Arctic waters between 1990 and 2012. *Climatic Change* 123:161–173, http://dx.doi.org/10.1007/s10584-013-1038-3.

Rignot, E., and P. Kanagaratnam. 2006. Changes in the velocity structure of the Greenland Ice Sheet. *Science* 311(5763):986–990, http://dx.doi.org/10.1126/science.1121381.

Rignot, E., and K. Steffen. 2008. Channelized bottom melting and stability of floating ice shelves. *Geophysical Research Letters* 35, L02503, http://dx.doi.org/10.1029/2007GL031765.

Savage, S.B. 2001. Aspects of iceberg drift and deterioration. Pp. 279–318 in *Geomophological Fluid Mechanics.* N.J. Balmforth and A. Provenzale, eds, Springer Verlag Press, Berlin.

Scambos, T., R. Ross, R. Bauer, Y. Yermolin, P. Skvarca, D. Long, J. Bohlander, and T. Haran. 2008. Calving and ice-shelf break-up processes investigated by proxy: Antarctic tabular iceberg evolution during northward drift. *Journal of Glaciology* 54:579–591, http://dx.doi.org/10.3189/002214308786570836.

Scambos, T., O. Sergienko, A. Sargent, D. MacAyeal, and J. Fastook. 2005. ICESat profiles of tabular iceberg margins and iceberg breakup at low latitudes. *Geophysical Research Letters* 32, L23S09, http://dx.doi.org/10.1029/2005GL023802.

Smith, K.L., A.D. Sherman, T.J. Shaw, and J. Sprintall. 2013. Icebergs as unique lagrangian ecosystems in polar seas. *Annual Review of Marine Science* 5:269–287, http://dx.doi.org/10.1146/annurev-marine-121211-172317.

Squire, V.A. 2007. Of ocean waves and sea-ice revisited. *Cold Regions Science and Technology* 49:110–133, http://dx.doi.org/10.1016/j.coldregions.2007.04.007.

Stern, A.A., E. Johnson, D.M. Holland, T.J.W. Wagner, P. Wadhams, R. Bates, E.P. Abrahamsen, K.W. Nicholls, A. Crawford, J. Gagnon, and others. 2015. Wind-driven upwelling around grounded tabular icebergs. *Journal of Geophysical Research* 120:5,820–5,835, http://dx.doi.org/10.1002/2015JC010805.

Tang, C.C.L., C.K. Ross, T. Yao, B. Petrie, B.M. DeTracey, and E. Dunlap. 2004. *The Circulation, Water Masses and Sea-Ice of Baffin Bay.* Report prepared for the Bedford Institute of Oceanography, Ocean Sciences Division, Dartmouth, Nova Scotia, 60 pp.

Todd, B.J., C.F.M. Lewis, and P.J.C. Ryall. 1988. Comparison of trends of iceberg scour marks with iceberg trajectories and evidence of paleocurrent trends on Saglek Bank, northern Labrador Shelf. *Canadian Journal of Earth Science* 24:1,374–1,883, http://dx.doi.org/10.1139/e88-132.

US Department of Commerce, National Oceanic and Atmospheric Administration, National Geophysical Data Center. 2006. 2-minute Gridded Global Relief Data (ETOPO2v2), http://www.ngdc.noaa.gov/mgg/fliers/06mgg01.html.

Van Wychen, W., and L. Copland. In press. Ice island drift mechanisms in the Canadian High Arctic. In *Arctic Ice Shelves and Ice Islands.* L. Copland and D. Mueller, eds, Springer, New York, New York.

Vernet, M., K.L. Smith Jr., A.O. Cefarelli, J.J. Helly, R.S. Kaufmann, H. Lin, D.G. Long, A.E. Murray, B.H. Robison, H.A. Ruhl, and others. 2012. Islands of ice: Influence of free-drifting Antarctic icebergs on pelagic marine ecosystems. *Oceanography* 25(3):38–39, http://dx.doi.org/10.5670/oceanog.2012.72.

Wagner, T.J.W., P. Wadhams, R. Bates, P. Elosegui, A. Stern, D. Vella, E.P. Abrahamsen, A. Crawford, and K.W. Nicholls. 2014. The "footloose" mechanism: Iceberg decay from hydrostatic stresses. *Geophysical Research Letters* 41:5,522–5,529, http://dx.doi.org/10.1002/2014GL060832.

ACKNOWLEDGMENTS

We would like to thank Luke Copland and the anonymous reviewers of this paper who provided valuable critiques that led to a greatly improved manuscript. We also thank all who were involved with PII-B data collection efforts. This includes Project Iceberg (the 2011 field campaign) members Andrew Hamilton, Alexander Forrest, Derek Mueller, Bernard Laval, Val Schmidt, and Richard Yeo. John Hughes Clarke and Danar Pratomo of the University of New Brunswick's Ocean Mapping Group are acknowledged for aiding with bathymetry data collection, while Jonathan Gagnon and Steeve Gagné are thanked for their on-ice support during 2012 fieldwork. Operation Iceberg was coordinated by Louise Ferguson, Laura Deponio, Andrew Thompson, Sarah Conner, and Heather Nicol of BBC Scotland. The captains and crews of CCGS *Amundsen* and M/V *Neptune* are acknowledged for their transportation and logistical support, as is Micheal O'Sullivan of Trinity Helicopters, and the employees of Arctic Kingdom, as well as Pedro Elosegui (CSIC/MIT) for GPS beacon support. Neither Project Icebergs nor Operation Iceberg would have been possible without the financial and in-kind support of the CIS (Leah Braithwaite with Environment Canada) and ArcticNet (Martin Fortier and Keith Levesque) for Project Icebergs and BBC Scotland (Mark Hedgecoe) for Operation Iceberg. Financial support was also provided by the Natural Science and Engineering Research Council, the Northern Scientific Training Program, and the Office of Naval Research Sea State Program. The interest and experience of Luc Desjardins, Ron Saper, and Gregory Crocker in ice island dynamics is greatly appreciated. Hai Train, Tom Carrieres, and Paul Pestieau are thanked for providing ablation modeling data from the Canadian Meteorological Centre. GPS beacons were provided by C-CORE (Tony King), the CIS, and Navidatum Ltd. (Tim Scott-Douglass). Finally, the research on PII-B would not be possible without the approval of the Nunavut Research Institute (Mosha Coté and Jamal Shirley, License #02 002 12R-M).

AUTHORS

Anna J. Crawford (anna.crawford@carleton.ca) is a PhD candidate in the Water and Ice Research Lab within the Department of Geography and Environmental Studies, Carleton University, Ottawa, Ontario, Canada. **Peter Wadhams** is Professor, Department of Applied Mathematics and Theoretical Physics, University of Cambridge, Cambridge, UK. **Till J.W. Wagner** is Postdoctoral Scholar, Scripps Institution of Oceanography, University of California San Diego, La Jolla, CA, USA. **Alon Stern** is Postdoctoral Scholar, Geophysical Fluid Dynamics Laboratory, Princeton University, Princeton, NJ, USA. **E. Povl Abrahamsen** is Research Scientist, British Antarctic Survey, Natural Environment Research Council, Cambridge, UK. **Ian Church** is Assistant Professor, Department of Geodesy and Geomatics Engineering, University of New Brunswick, Fredericton, NB, Canada. **Richard Bates** is Senior Lecturer and Research Scientist, University of Saint Andrews, Saint Andrews, UK. **Keith W. Nicholls** is Research Scientist, British Antarctic Survey, Natural Environment Research Council, Cambridge, UK.

ARTICLE CITATION

Crawford, A.J., P. Wadhams, T.J.W. Wagner, A. Stern, E.P. Abrahamsen, I. Church, R. Bates, and K.W. Nicholls. 2016. Journey of an Arctic ice island. *Oceanography* 29(2):254–263, http://dx.doi.org/10.5670/oceanog.2016.30.